

A Second Order 3D BEM for Wave-Structure Interaction

Jesper Skourup¹, Bjarne Büchmann² & Harry B. Bingham¹

INTRODUCTION

At the previous workshop a 3D Boundary Element Model with active absorption at the open boundaries was presented. The model was formulated correct to second order in the free surface conditions but only the linear part of it was implemented. The tests involved regular waves on a fixed structure and forced linear motions of a floating structure. Further details can be found in Skourup and Bingham (1996).

The present abstract considers some of the extensions to the model, which have been implemented since the last workshop. The second order free surface conditions have now been implemented and active absorption is used at the lateral boundaries for both the first order scattered waves and for the second order scattered waves. Numerical results to second order of the run-up on a fixed vertical circular cylinder are presented and they agree well with the analytical second order results by Kriebel (1992). Results are also presented using first order irregular waves incident on a freely floating ship. The computed motions of the ship compare well with linearized frequency domain calculations using the well verified frequency domain code WAMIT.

MATHEMATICAL FORMULATION

A potential flow is assumed, with boundary conditions expanded up to second order and applied on the mean positions of the free surface and body boundaries (see Isaacson and Cheung, 1992, or Skourup, 1996). The total velocity potential is separated into a known incident potential ϕ_I , and a scattering potential ϕ_S representing the effects of the body and its motions,

$$\phi(\vec{x}, t) = \varepsilon \left[\phi_I^{(1)}(\vec{x}, t) + \phi_S^{(1)}(\vec{x}, t) \right] + \varepsilon^2 \left[\phi_I^{(2)}(\vec{x}, t) + \phi_S^{(2)}(\vec{x}, t) \right] + \dots \quad (1)$$

where ε is the perturbation parameter, \vec{x} is an observation point, t is the time and the superscripts denote the order of the expansion. By formulating the boundary value problem for the scattered field alone all waves in the domain are outgoing waves, and all lateral boundaries can thus be formulated as absorbing boundaries.

The active wave absorption method used here is similar to the one used at the Danish Hydraulic Institute for wave absorption in physical flumes. The motion of a wave absorber is a function of the time history of the wave absorber position and of the free surface elevation at the wave absorber. These are transformed to an updated wave absorber position by use of a digital filter designed to match a theoretically determined transfer function (see Schäffer et al., 1994, for details). The same technique may also be used in a 3D model by considering a finite number of 2D wave absorbers placed next to each other and working independently. Each absorber is then governed by the same digital recursive filter and by the local time history of the position of the absorber and the elevation there. An extension to a fully 3D active absorption method is given in Schäffer and Skourup (1996), but it has not yet been implemented

¹ International Research Centre for Computational Hydrodynamics, Danish Hydraulic Institute, Agern Allé 5, DK-2970 Hørsholm, Denmark, e-mail:icch@dhi.dk

² Department of Hydrodynamics and Water Resources, Building 115, Technical University of Denmark, DK-2800 Lyngby, Denmark, e-mail:buchmann@isva.dtu.dk

into the present version of the program. In the numerical simulations the absorbers all work in the piston mode, but digital filters are also available for hinged flap wave absorbers. The wave absorber boundary condition is of the Neumann type.

To compute the potential, the boundary value problem is re-cast as a boundary integral equation via Green's 2nd identity

$$\alpha(\bar{x})\phi(\bar{x}, t) = \int_{\Gamma} \phi(\bar{\xi}, t)G_n(\bar{x}, \bar{\xi}) - G(\bar{x}, \bar{\xi})\phi_n(\bar{\xi}, t) d\Gamma \quad (2)$$

where $\bar{\xi} = (\xi_1, \xi_2, \xi_3)$ is the position vector of an integration point situated at the boundary Γ of the domain, subscript n indicates differentiation along the outwards normal vector at $\bar{\xi}$, and the factor $\alpha(\bar{x})$ depends on the position of the observation point ($\alpha(\bar{x}) = 2\pi$ for \bar{x} situated at a smooth part of the boundary).

Equation (2) is discretized using a panel method with the kernel function $G(\bar{x}, \bar{\xi}) = 1/|\bar{x} - \bar{\xi}|$, and the variation over a panel of both the potential and the geometry is taken to be linear. Collocation is performed at the corners of each panel, and the resulting linear system of equations is solved by LU factorisation at the first time level (i.e. at $t=0$) and then by back-substitution at each time step. The free surface boundary conditions are integrated using 4th order Adams-Bashforth and Adams-Moulton schemes. Further details concerning the numerical solution can be found in Skourup (1996).

NUMERICAL EXAMPLES

Two numerical examples are given in this abstract. The first example considers second order wave run-up on a fixed vertical circular cylinder. The numerical wave tank is square with a side length equal to about 3.5 times the length of the regular waves used in each test. The cylinder is situated with the centre at the symmetry line of the wave tank, and a Green's function accounting for the symmetry and satisfying the impermeability condition at the horizontal sea bed is used. Thus, the calculation domain can be reduced to half of the original domain and the sea bed can be excluded. For these tests the boundary of the domain is discretized using about 3500 nodes and a simulation covering 10 wave periods is performed using 2000 time steps. The computing time for one simulation is 40 CPU minutes on an IBM RS6000 computer.

The maximum run-up on the cylinder is determined as the average value of the wave crest height during a few wave cycles. The linear solution is well known and straightforward to compute (cf. MacCamy and Fuchs, 1954), while the second order solution is by no means simple to determine (see Kriebel, 1990). Kriebel (1992) gave results correct to second order for wave run-up on a vertical circular cylinder covering a range of ka and kh values (where k is the wavenumber, a is the cylinder radius and h is the water depth). These results are reproduced using the present second order Boundary Element Method. In Fig. 1 $ka=0.271$, $kh=0.750$ and the wave steepness is $kH=0.215$ (where H is the wave height). The agreement with the second order run-up curve from Kriebel (1992) is very good. Another example with $ka=0.684$, $kh=1.894$ and $kH=0.391$ is depicted in Fig. 2. Again the agreement with the results by Kriebel (1992) is excellent. A more comprehensive comparison with Kriebel's results will be given at the conference.

As a second example we consider a Series 60 $C_b=0.7$ hull exposed to a sum of first order waves (corresponding to an irregular wave time series) incident from ahead. In order to minimize wave reflections (i.e. by generating waves in the optimal frequency range of the active absorber), and to retain an adequate spatial discretization for all wave components, eight waves distributed in the range $1.29 < \omega' < 2.48$ are used (where $\omega' = \omega\sqrt{h/g}$ is the non-dimensional radian wave frequency). The boundary of the domain is discretized with 2000 nodes and a simulation covering 2048 timesteps takes about 15 CPU minutes on the IBM RS6000 computer. Figures 3, 4 and 5 show the response amplitude operators (RAO) and phases for the ship in the surge, heave and pitch modes. These results have been computed as the Fourier transform of the body motion relative to the Fourier transform of the incident wave elevation at the centre of the ship. The simulation results compare well with calculations made using the well verified frequency-domain code WAMIT (1995). The small discrepancies at the higher frequencies are attributed to a sparse discretization of the corresponding wave lengths.

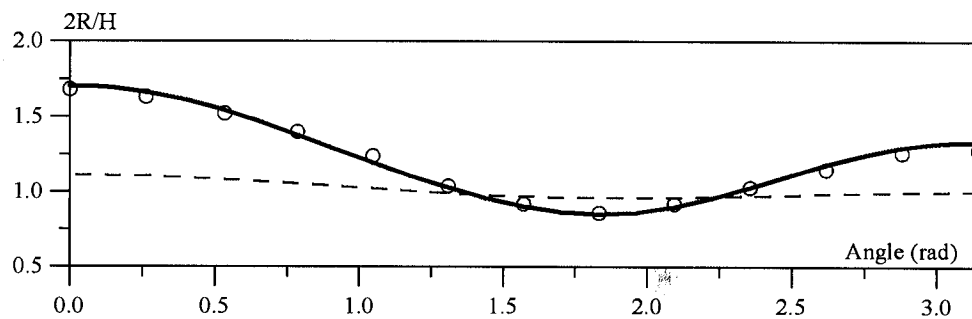


Figure 1. Wave run-up on fixed vertical circular cylinder. $ka=0.271$, $kh=0.750$, $kH=0.215$. Linear solution (dashed), second order solution (solid). The analytical results by Kriebel (1992) are depicted by circles.

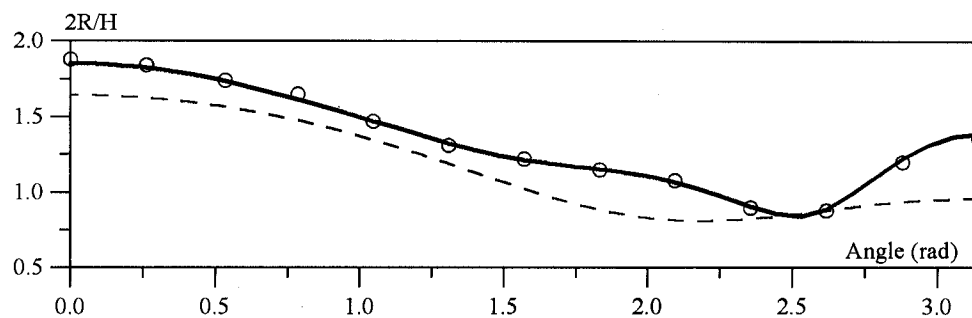


Figure 2. Wave run-up on fixed vertical circular cylinder. $ka=0.684$, $kh=1.894$ and $kH=0.391$. Linear solution (dashed), second order solution (solid). The analytical results by Kriebel (1992) are depicted by circles.

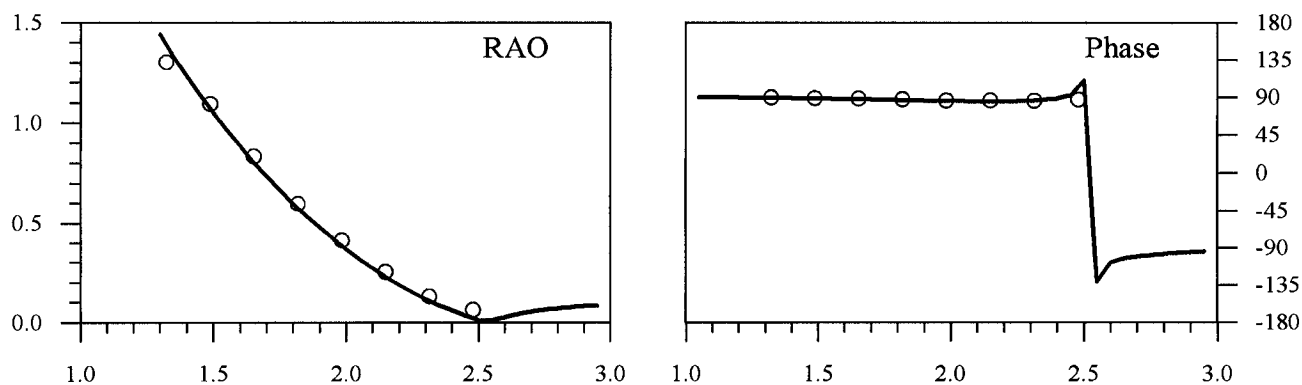


Figure 3. Surge RAO and phase (in degrees) for a Series 60 hull ($C_b=0.7$) exposed to irregular waves. The non-dimensional radian wave frequency ω' is depicted on the x-axis, the WAMIT results are shown with a solid line and the present numerical results are depicted by circles.

CONCLUSIONS

A second order 3D Boundary Element Model for the interaction between waves and structures has been developed. For a fixed structure (vertical circular cylinder) the wave run-up correct to second order has been computed, and the numerical results agree well with the analytical solution by Kriebel (1990,1992). The interaction between irregular waves and a freely floating ship has been simulated using the linear part of the model and good agreement with the theoretical RAOs and phases are found.

The interaction between waves, a current and a structure is also implemented and can be simulated by the present model. Results with the interaction of waves, current and a structure will be shown at the conference, but published elsewhere (see Büchmann et al., 1997).

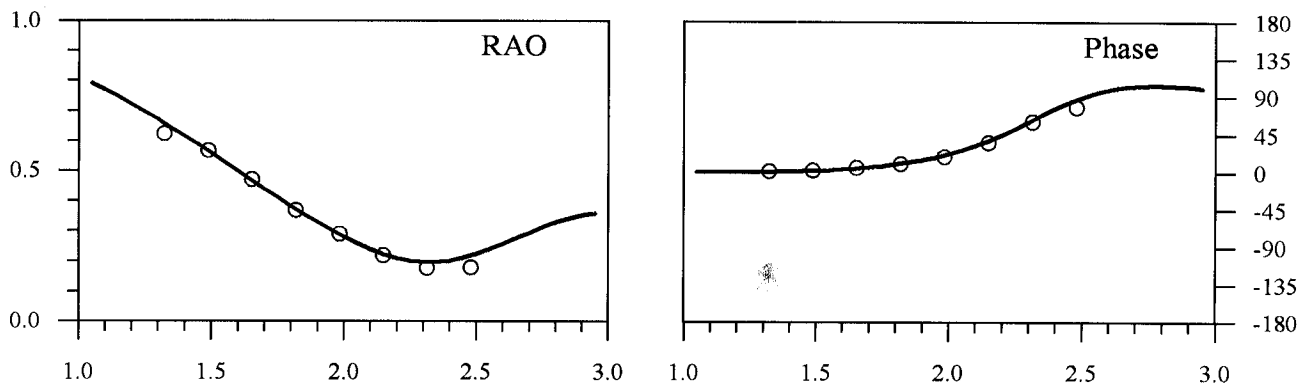


Figure 4. Heave RAO and phase (in degrees) for a Series 60 hull ($C_b=0.7$) exposed to irregular waves. The non-dimensional radian wave frequency ω' is depicted on the x-axis, the WAMIT results are shown with a solid line and the present numerical results are depicted by circles.

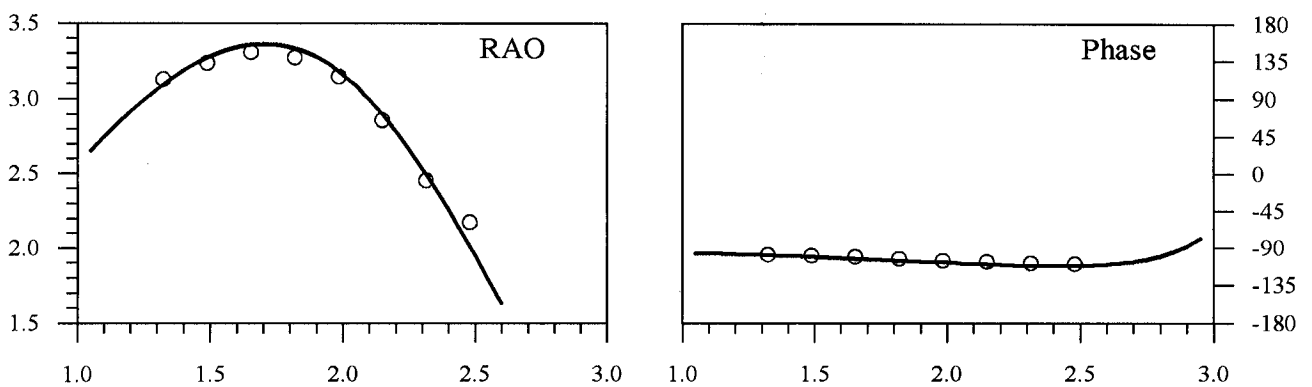


Figure 5. Pitch RAO and phase (in degrees) for a Series 60 hull ($C_b=0.7$) exposed to irregular waves. The non-dimensional radian wave frequency ω' is depicted on the x-axis, the WAMIT results are shown with a solid line and the present numerical results are depicted by circles.

ACKNOWLEDGEMENTS

The present work was funded by the Danish National Research Foundation. Their support is greatly appreciated. David L. Kriebel is thanked for sending us the analytical second order runup data.

REFERENCES

- Büchmann, B., Skourup, J. and Cheung, K.F. (1997). Runup on a structure due to waves and a current. To be presented at the 7th Int. Offshore and Polar Engineering Conf. (ISOPE-97), Honolulu, Hawaii, USA.
- Isaacson, M. and Cheung, K.F. (1992). Time-domain second-order wave diffraction in three dimensions. *Journal of Waterway, Port, Coastal and Ocean Engineering*, ASCE, **118**(5), 496-515.
- Kriebel, D.L. (1990). Non-linear wave interaction with a vertical circular cylinder. Part I: Diffraction theory. *Ocean Engineering*, **17**(4), 345-377.
- Kriebel, D.L. (1992). Non-linear wave interaction with a vertical circular cylinder. Part II: Wave run-up. *Ocean Engineering*, **19**(1), 75-99.
- MacCamy, R.C. and Fuchs, R.A. (1954). Wave forces on piles: a diffraction theory. U.S. Army Corps of Engineers, *Beach Erosion Board*, Tech. Memo. No. 69, Washington D.C.
- Schäffer, H.A., Stolborg, T. and Hyllested, P. (1994). Simultaneous generation and active absorption of waves in flumes. Proc. of the Int. Symp.: WAVES - Physical and Numerical Modelling, Vancouver, Canada, 90-99.
- Schäffer, H.A. and Skourup, J. (1996). Active absorption of multi-directional waves. Proc. of the 25th Int. Conf. on Coastal Engineering. Orlando, Florida, USA.
- Skourup, J. (1996). Active absorption in a numerical wave tank. Proc. of the 6th Int. Offshore and Polar Engineering Conf. (ISOPE-96), Los Angeles, USA, vol. 3, 31-38.
- Skourup, J. and Bingham, H.B. (1996). Active absorption of radiated waves in a 3D boundary element model. Proc. of the 11th Int. Workshop on Water Waves and Floating Bodies. Hamburg, Germany.
- WAMIT (1995). User Manual. Department of Ocean Engineering, Massachusetts Institute of Technology.